Excitation of the $B\,^3\Pi_g$ states of N_2 by electron impact*

S. T. Chen and R. J. Anderson
Department of Physics, University of Arkansas, Fayetteville, Arkansas 72701
(Received 24 December 1974; revised manuscript received 18 March 1975)

Radiative lifetime measurements of 13 vibrational levels of the $B\,^3\Pi_g$ state of N_2 have been obtained at 50 eV incident electron energy and 30 mTorr N_2 gas pressure using a 50-μsec electron excitation pulse. Two radiative decay components with lifetimes of approximately 5 and 25 μsec are observed in each case. The short-lived component is identified as the contribution from direct excitation of the $B\,^3\Pi_g$ state. The long-lived cascade contribution is observed to decrease from 37% of the total $B\,^3\Pi_g \rightarrow A\ ^3\Sigma_u^+(v',v'')$ radiation for the $v'=0$ vibrational level to 15% for the $v'=12$ level and is consistent with theoretical predictions by Cartwright *et al.*

I. INTRODUCTION

Electron-N_2 collision processes have particular significance in terrestrial atmospheric science because of the abundance of molecular nitrogen in Earth's atmosphere. A knowledge of absolute transition probabilities and lifetimes for the electronic transitions of N_2 is also important in many problems in astrophysics, plasma physics, chemical kinetics, and laser studies. In the present experiment, time-resolved spectroscopy has been used to study electron-impact excitation of the $B\,^3\Pi_g$ states of N_2. Lifetime measurements of 13 vibrational levels of the $B\,^3\Pi_g$ electronic state are obtained by observing the temporal decay of the first-positive band system corresponding to $B\,^3\Pi_g \rightarrow A^3\Sigma_u^+(v', v'')$ transitions. (A partial energy-level diagram of N_2 and N_2^+ is shown in Fig. 1.)

Several investigators[1-3] have previously measured the lifetimes of vibrational levels of the $B\,^3\Pi_g$ state of N_2. In addition, Chung and Lin[4] have calculated the electron-impact excitation cross sections of the $B\,^3\Pi_g$ state and found that the calculated cross sections were about one-half that of the experimental apparent cross sections[5,6] corrected for cascade from the $C\,^3\Pi_u$ state. Meanwhile, theoretical calculations by Cartwright *et al.*[7,8] indicate that radiative cascade from higher vibrational levels of the $W\,^3\Delta_u$ and $A^3\Sigma_u^+$ states could play a significant role in populating the lower vibrational levels of the $B\,^3\Pi_g$ state and hence change the character of its apparent excitation cross sections. In the present work, lifetime measurements of 13 vibrational levels ($v'=0-12$) of the $B\,^3\Pi_g$ state are obtained at 50-eV electron impact energy, 50-μsec electron excitation pulse width, and 30-mTorr N_2 gas pressure. A significant long-lived cascade contribution is observed for each vibrational level and is consistent with theoretical predictions by Cartwright *et al.*[7,8]

II. EXPERIMENT

A. Apparatus

The experimental apparatus shown in Fig. 2 utilizes a version of time-resolved spectroscopy developed at the University of Arkansas.[9] Spectroscopically pure nitrogen gas passes into the excitation chamber through a VACOA precision gas-metering valve. The gas flow is held at a constant

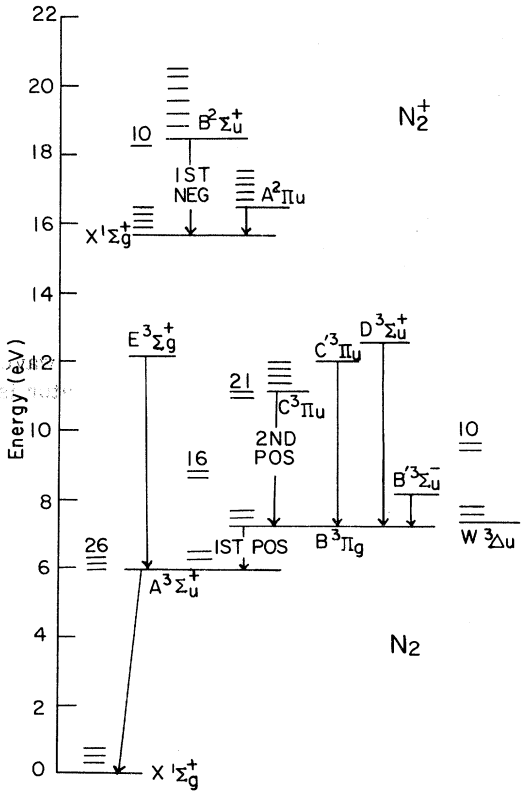

FIG. 1. Partial energy-level diagram of N_2 and N_2^+.

rate, corresponding to a N_2-target-gas pressure of 30 mTorr. The N_2 gas pressure is measured by means of a well-trapped McLeod gauge while the residual background pressure is determined to be ~10^{-6} Torr by means of a calibrated ion gauge.

A 6EM5 beam-power tube of pentode design is used to produce a gated electron beam which acts as the primary excitation mechanism. The pulsed electron beam has an incident energy of 50 eV, a peak current of 0.01 A, a duration of 50 μsec, a repetition rate of ~2 kHz, and a cutoff time of less than 7 nsec. The energy distribution of the electron beam was determined as ≤ 5 eV by means of the retarding-potential method. The pulsed electron beam passes into a field-free excitation region through a 0.3-cm-wide by 1.8-cm-long slit and is collected in a deep cylindrical Faraday cup (6 cm in length, 4.3 cm in diameter). The excitation region is surrounded on three sides by electrically grounded walls producing an effective excitation chamber of dimensions 2 cm length $\times$ 2.5 cm width $\times$ 2 cm height. The modulated light signal passes out of the collision chamber at a right angle to the electron beam through a 1-in.-diam quartz window placed immediately adjacent to the excitation region.

The collisional radiation is directed into one of two alternate optical analyzing systems. The first system consists of a lens to focus the light, with unit magnification parallel to the entrance slit of a plane-grating monochromator. A photomultiplier tube is placed at the exit slit of the monochromator to detect the light corresponding to the spectral transition under study. A Jarrell-Ash 0.5-m scanning monochromator with a grating blazed at 6000 Å and operated at a spectral resolution of 8 Å is used to isolate the spectrum in the region below $\lambda = 8000$ Å. In the case of longer wavelengths, a Jarrell-Ash 0.25-m monochromator is used. The latter instrument contains a grating blazed at 1.3 μm and is operated at a spectral resolution of 33 Å. Two photomultiplier tubes, an Amperex 56 TVP and a RCA 7102, are used to monitor the spectral range from about $\lambda = 5700$ Å to $\lambda = 10\,600$ Å. The RCA 7102 photomultiplier tube is cooled to dry-ice temperature, thereby reducing the dark current by a factor of 15. Combinations of colored-glass transmission filters placed after the collision-chamber window are used to block unwanted second and third spectral orders. In this manner transmission of light at wavelengths below $\lambda = 5200$ Å is reduced to less than 1% of its normal value. Meanwhile, more than 98% of the longer-wavelength light is transmitted through the filter combinations. The second analyzing system consists of a lens to render the diverging light from the electron-beam excitation region into parallel rays, a Baird atomic type B-9 infrared interference filter (transmission bandpass $\Delta\lambda = \pm 100$ Å), and a second lens to focus the light onto a cooled RCA 7102 photomultiplier tube with unit magnification.

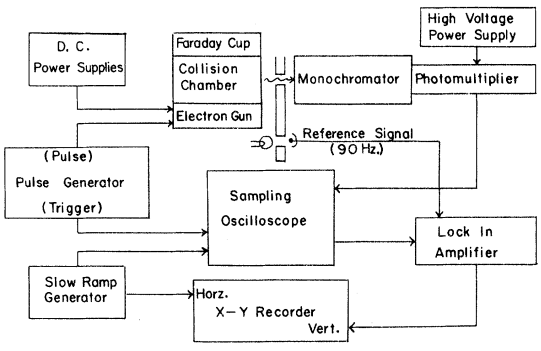

FIG. 2. Block diagram of the experimental apparatus.

The time-resolved photodetection system employs a sampling oscilloscope to analyze the decay of the collisional radiation. The signal-to-noise ratio of the sampling system is improved by a factor of ~5 by use of a double-modulation detection scheme in which the 2-kHz pulsed collisional radiation is modulated a second time at 85 Hz by a mechanical chopper. The normally dc output of the sampling oscilloscope therefore becomes a modulated output which can be monitored by a lock-in detector before being displayed on an x-y recorder. The use of the lock-in detector tends to reduce the uncertainties introduced into the decay signal by noise and dc amplifier drift present in the sampling unit. The resulting x-y trace is a plot of light intensity versus time. The lock-in detector signal is normalized to correspond to the maximum vertical deflection of the recorder, while the horizontal time axis is placed on an absolute scale by monitoring a signal of known frequency with the sampling system. Typical rms signal-to-noise ratios for the decay curves lie in the range ~8–100 for the maximum amplitude of the curve occurring before the excitation cutoff and ~0.5–50 for the minimum amplitude occurring several lifetimes after the cutoff time. The minimum response time of the system was determined to be in the range 3–7 nsec,[10] a time interval much shorter than the $B^3\Pi_g$ lifetimes under study.

B. Data analysis

The lifetimes of 13 vibrational levels ($v' = 0 - 12$) of the $B^3\Pi_g$ state of N_2 are measured by observing the first-positive band system corresponding to

the $B^3\Pi_g \rightarrow A^3\Sigma_u^+$ transitions. Relative-intensity–versus–wavelength graphs of the N_2 spectrum excited by a 50-eV dc electron beam at a N_2 gas pressure of 30 mTorr are shown in Fig. 3. The wavelength scans are obtained at spectral resolutions of 8 and 33 Å for the wavelength regions $\lambda = 5700$–6900 Å and $\lambda = 8600$–$10\,600$ Å, respectively. The intensities displayed in Fig. 3 are not corrected for differences in detector sensitivity and are shown to indicate that although there exists considerable overlapping of the first-positive spectral bands in the $\Delta v' = 4$ sequence, the overlapping of bands diminishes as $\Delta v'$ decreases until finally at $\Delta v' \leq 1$ the bands are well separated. In the present experiment, all of the lifetime measurements except that of the $(v' = 0 \rightarrow v'' = 0)$ transition are obtained with the central transmission wavelength of the monochromator set at the maximum intensity feature of each band and at the previously indicated spectral resolution. In the case of the $(v' = 0 \rightarrow v'' = 0)$ transition the $\lambda = 10\,500$ Å spectral band is isolated by means of an infrared-transmission filter. In addition, the $v' = 2 \rightarrow v'' = 1)$ lifetime measurement is also obtained using a filter-analyzing system to examine the effects of the optical field of view upon the measurements.

The observed radiative decay curve corresponding to each $B^3\Pi_g$ vibrational level is analyzed as a superposition of exponential decays. The instantaneous light intensity is expressed as

$$\frac{I(t)}{I(t=0)} = \sum_j C_j e^{-A_j t} , \qquad (1)$$

where C_j and A_j are, respectively, the amplitude and the radiative-decay constant of the jth component, and $\sum_j C_j = 1$. The unknown parameters, C_j and A_j, are determined by a least-squares analysis of the experimental data. The computer program used to analyze the radiative lifetime data obtained in the present experiment is the BMDX85 nonlinear least-squares fit.[11] It obtains a least-squares fit of the function $I(t)/I(t=0)$ to the data values t_i by means of stepwise Gauss-Newton iterations on the initial estimates of C_j and A_j obtained by graphical analysis of the radiative-decay curve. The computer-program output includes the last-fitted parameters, estimates of fitting errors, the original data, and the computer-generated fit to the experimental data. For each vibrational transition the data from at least ten individual decay curves are included in the computer analysis. Values of C_j and A_j are computed, corresponding mean values are obtained, and standard deviations of the respective mean values are calculated. The over-all experimental error present in the measurements of C_j and A_j is estimated to be within ±20%. Our estimate considers errors introduced by (a) the experimental technique, (b) the analysis of the x-y recorder plot, and (c) the computer fit.

Analysis of the $B^3\Pi_g \rightarrow A^3\Sigma_u^+$ radiative-decay curves yields a short-lived decay constant of $\sim 2.5 \times 10^5$ sec^{-1}, and a long-lived component corresponding to a second decay constant of $\sim 4 \times 10^4$ sec^{-1}. The larger decay constant is identified as the sum of the $B^3\Pi_g$-state natural-decay constant and the decay constants corresponding to competing excitation processes. The natural lifetime of the $B^3\Pi_g$ state is the inverse of this sum after the latter contributions have been subtracted from the total. The second decay constant is associated

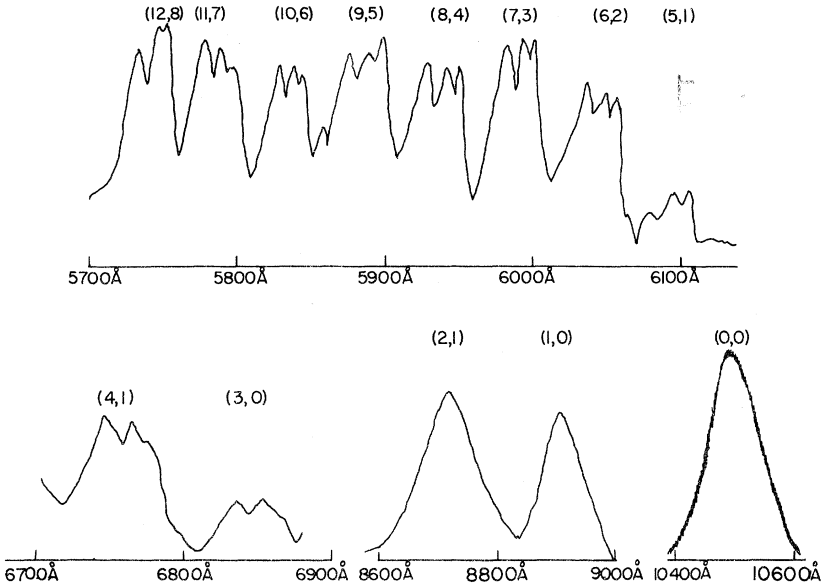

FIG. 3. Relative photomultiplier signal-vs-wavelength scan of N_2 spectrum indicating freedom of spectrum overlap as $\Delta v'$ decreases: PMT signal uncorrected for differences in detector spectral efficiency.

with the population of the $B^3\Pi_g$ states by radiative cascade from other electronic states and also is affected by competing excitation processes. These assumptions concerning the origins of the decay modes and the effects of secondary excitation and deexcitation processes upon the decay constants will be discussed in detail in Sec. III. A computer-generated semilogarithmic plot of a typical radiative decay curve is shown in Fig. 4.

III. RESULTS AND DISCUSSION

A. Secondary excitation processes

The secondary excitation and deexcitation processes considered in the present analysis of the $B^3\Pi_g \rightarrow A^3\Sigma_u^+$ radiative decay are (i) population by radiative cascade, (ii) wall-collisional depopulation controlled by diffusion, and (iii) volume-collisional depopulation. Other secondary population processes such as radiation imprisonment and collisional excitation of ground-state molecules are neglected in the present analysis because of the relatively low concentrations of excited-state molecules produced under the present experimental conditions.

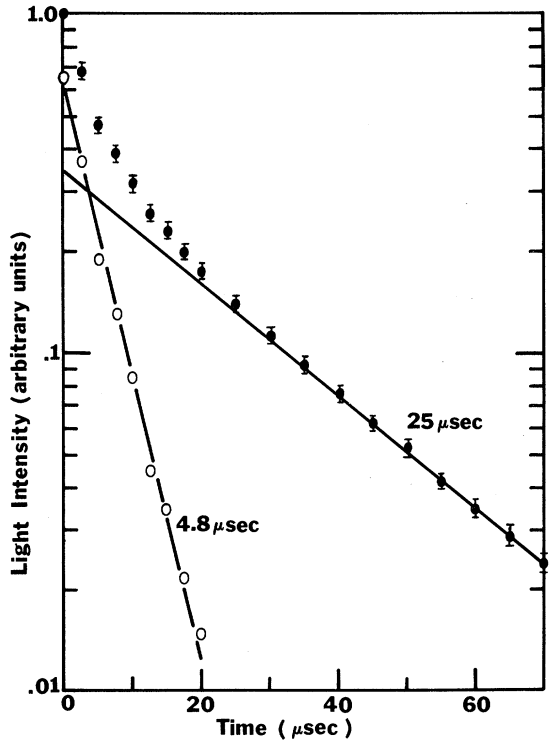

FIG. 4. Computer-generated semilogarithmic plot of light intensity versus time for the $\lambda = 8722$ Å band corresponding to the (2,1) transition of the N_2 first positive system observed with a monochromator analyzing system: error bars indicate reproducibility and reading errors present in the data acquisition process.

The present experiment was conducted at a N_2 gas pressure of 30 mTorr and an estimated operating temperature of 600 °K. Under these conditions the ground-state molecular density (ρ) is approximately 5×10^{14} molecules/cm^3, the average molecular velocity ($\bar{v}$) is calculated to be 6.7×10^4 cm/sec, the concentration of $B^3\Pi_g$ states produced by direct excitation during the 0.01-A–50-μsec electron pulse is estimated to be ~10^9 molecules/cm^3 and the gas-kinetic collision time is estimated to be comparable to the $B^3\Pi_g$ lifetime. Because of this latter fact, it is important that the effects of volume-collisional depopulation upon the $B^3\Pi_g$ radiative-decay constant be investigated. The volume-collisional contribution to the observed decay constant is given by the product $\rho\bar{v}\sigma$, where σ is the effective collisional cross section for volume depopulation of the $B^3\Pi_g$ state. Using the value $\sigma \simeq 3\times10^{-16}$ cm^2 reported by Johnson and Fowler,[3] the collisional contribution to the $B^3\Pi_g$ decay constant is estimated to be 1×10^4 sec^{-1}, which is ~4% of the total and within the experimental error of the present investigation.

The diffusion of excited-state molecules affects the radiative-decay analysis in two ways: (a) wall-collisional depopulation controlled by diffusion and (b) removal of the excited states from the field of view of the optical system before their decay is detected. The latter process would appear to be especially significant when the optical field of view is restricted, as in the case of the monochromator analyzing system.

In the present experiment the diffusion time constant (τ) is calculated for the geometry of a parallelpiped whose sides a, b, and c correspond to the dimensions of the optical field of view. When an optical interference filter is used to isolate the collisional radiation, the field of view of the optical system is determined by the dimensions of the exit window (~2.5-cm diam), the filter (~2.5-cm diam), and the photocathode (~3-cm diam). In this case the field of view is much larger than the width of the electron beam and comparable to the dimensions of the excitation chamber. Under these conditions wall-collisional depopulation may affect the measured decay constant. The diffusion constant (D), reported by Winter,[12] and the dimensions of the excitation chamber are used in the formula,[13]

$$\frac{1}{\tau} = \pi^2 D\left[\left(\frac{1}{a}\right)^2 + \left(\frac{1}{b}\right)^2 + \left(\frac{1}{c}\right)^2\right]$$

to obtain an estimate of the amount that wall-collisional depopulation contributes to the observed

decay constants. The wall-collisional depopulation mechanism accounts for approximately 4% of the $B^3\Pi_g$-state total decay constant and up to 22% of the decay constant representing the long-lived decay.

In the case of the monochromator analyzing system, the optical field of view is determined by the width of the monochromator entrance slit ($\leq$1 mm). The diffusion time for an excited state to leave the 1-mm section of the electron beam viewed by the monochromator analyzing system is calculated to be 1.8×10^{-7} sec. Therefore, there exists the possibility that excited-state molecules will diffuse out of the optical field of view before their decay is detected. However, because the ratio of the electron beam width to the field of view is large ($\geq$ 4), there also exists the possibility that similar excited molecules may diffuse into the field of view as they decay. This assumption is supported by the fact that lifetime measurements carried out on the ($v'=2\rightarrow v''=1$) transition with both filter and monochromator analyzing systems produced the same values of the two decay constants to within the reported experimental error. In addition, the amplitudes C_1 and C_2 determined by analysis of the semilogarithmic decay plot are observed to be independent of the type of optical analyzing system used in the measurement. These facts appear to indicate that the effects of diffusion processes upon the excited-state decay constant and relative population lies within our experimental error and cannot be accurately determined. Therefore, the effects of excited-state diffusion will be neglected in the following analysis of the $B^3\Pi_g$ population decay.

The remaining secondary excitation mechanism which can play an important role in populating the $B^3\Pi_g$ state is radiative cascade. In particular, the present work will investigate the apparent long-lived decay component (~25 μsec) observed in the time-resolved spectra of the $B^3\Pi_g\rightarrow A^3\Sigma_u^+$ transition. The analysis will be carried out assuming (i) that the only secondary processes of importance are radiative cascade and volume-collisional depopulation of the $B^3\Pi_g$ vibrational levels and (ii) that the vibrational levels of the several electronic states which can experience radiative cascade to the $B^3\Pi_g$ state are populated only by direct excitation. Under these assumptions, the constants C_j and A_j appearing in Eq. (1) can be identified as follows:

$$A_1 = 1/\tau_1 + \rho\sigma v, \quad A_2 = 1/\tau_2 ,$$

$$C_1 = N_1^* - C_2\frac{\tau_1}{\tau_2}, \quad C_2 = \frac{1-N_1^*}{1-\tau_1/\tau_2} ,$$

where τ_1 is the natural lifetime of the $B^3\Pi_g$ state, τ_2 is the effective lifetime of the group of states which experience radiative cascade to the $B^3\Pi_g$ state, N_1^* is the fraction of the total $B^3\Pi_g$ population resulting from direct excitation, and $1-N_1^*$ is the $B^3\Pi_g$-state population fraction resulting from radiative cascade transitions.

B. $B^3\Pi_g$-state lifetime measurements

In Table I, the results of the present measurements of the $B^3\Pi_g$ lifetimes are compared with those reported by Jeunehomme[1] and by Johnson and Fowler (JF).[3] In the JF experiment, a short-excitation electron pulse (i.e., pulse width between two and three times that of the $B^3\Pi_g$ lifetime) was used to minimize the population of possible long-lived excited states. Although JF measured the $B^3\Pi_g$ lifetime as a function of N_2 gas pressure and extrapolated to zero pressure to obtain the natural lifetimes given in Table I, the lowest pressure at which they carried out measurements is comparable to the 30-mTorr gas pressure used in the present experiment. In addition, JF did not observe a significant pressure dependence of the $B^3\Pi_g$-state lifetimes at gas pressures below ~200 mTorr. Therefore, the present results and those of JF appear to be in reasonable agreement, especially considering the ±25% errors reported by JF and the ~± 20% errors estimated in this work. In a somewhat different approach, Jeunehomme[1] used a pulsed rf discharge as the excitation mechanism to obtain measurements of the $B^3\Pi_g$ lifetimes over a pressure range of 4–50 mTorr and extrapolated his results to zero pressure to obtain estimates of the natural lifetimes. His results are displayed in Table I as $\tau(J)$ at zero pressure.

C. Cascade analysis

The average lifetimes and fractions of the long-lived cascade contribution for each of the 13 vibrational levels of the $B^3\Pi_g$ state measured in the present experiment are summarized in Table I. The long-lived cascade contribution from higher levels to the $B^3\Pi_g$ state is observed to decrease from 37% of the total $B^3\Pi_g$ ($v'=0$) population to 15% for the $B^3\Pi_g$ ($v'=12$) level. Jeunehomme[1] also analyzed the observed $B^3\Pi_g\rightarrow A^3\Sigma_u^+$ light decay as a superposition of several exponential decays. The computer analysis of the $v'=7$ vibrational level of the $B^3\Pi_g$ state is examined as an example of the two experimental procedures. The results of the least-squares computer fit assuming a two-mode decay model carried out by Jeunehomme[1] yields $\tau_1 = 6.00\pm1.56$ μsec, $\tau_2 = 25.10\pm3.97$ μsec, $C_1 = (73.66\pm10.04)\%$, and $C_2 = (26.34\pm9.69)\%$. These values are compared to the present results of

TABLE I. $B\,^3\Pi_g$ lifetime data.

Vibrational level (v)	$B\,^3\Pi_g$ lifetimes τ_1 (this work) [b] (μsec)	τ(JF) [c] (μsec)	τ(J) [d] (μsec)	Long-lived cascade contribution observed in the present experiment [a] τ_2 (μsec)	% of long-lived cascade
0	4.9±0.5		8.0	23.5±2.0	37.1±7.2
1	4.5±0.5		7.5	25.1±4.6	37.3±3.8
2	4.6±0.7		7.1	25.0±2.0	34.2±5.2
3	4.7±0.4	3.3	6.8	24.9±2.8	36.1±3.0
4	5.5±0.4	4.0	6.5	26.0±1.4	33.1±3.6
5	5.1±0.8	3.5	6.2	24.2±1.7	32.3±5.3
6	5.5±0.8	4.0	6.0	23.7±3.2	33.4±7.8
7	5.0±0.5	4.3	5.3	23.6±1.6	30.3±6.1
8	4.5±0.5	4.0	5.1	20.8±2.2	29.0±5.6
9	4.0±0.4		4.8	21.2±2.4	27.5±3.1
10	5.1±0.2		4.4	23.6±1.2	23.4±3.2
11	4.9±0.4			23.8±2.2	20.7±1.5
12	5.0±0.2			23.5±2.6	15.3±1.5

[a] Lifetime of long-lived cascade contribution uncorrected for volume and wall collisional depopulation.

[b] $B\,^3\Pi_g$ lifetime measured at 30 mTorr and corrected for the effects of volume-collisional depopulation: The errors represent the standard deviation of the mean lifetimes obtained by computer analysis of ten radiative decay curves.

[c] $B\,^3\Pi_g$ lifetime obtained by extrapolation to zero pressure by JF (Ref. 3).

[d] $B\,^3\Pi_g$ lifetime obtained by extrapolation to zero pressure by Jeunehomme (Ref. 1).

$\tau_1 = 5.0 \pm 0.5$ μsec, $\tau_2 = 23.6 \pm 1.6$ μsec, $C_1 = (62 \pm 6)\%$, and are observed to exhibit good agreement to within the reported experimental errors.

Several papers[4,7,8,14,15] have previously commented on the origin of the long-lived cascade contribution to the $B^3\Pi_g$ state. Benesch and Saum[15] have studied the $W \rightarrow B$ and $B \rightarrow W$ transitions and concluded that the intrasystem cascading effect is important in the $W \rightleftarrows B$ process, i.e., the $W \rightarrow B$ process must contribute, at least to some degree, in the emission of the first-positive band system. In principle, intrasystem cascading can occur in band systems where the vibrational levels of one state at least partly overlap those of another. Gilmore[14] has pointed out that the Franck-Condon factors of the $A^3\Sigma_u^+$ state favor excitation to the vibrational levels around $v' = 10$. These levels can make radiative transitions to the lower vibrational levels of the $B^3\Pi_g$ state, which then experience radiative transitions to the $A^3\Sigma_u^+$ state with the emission of the first-positive bands. Cartwright *et al.*[7,8] used electron-impact-excitation cross sections for the six lowest triplet states (A, B, W, C, E, D) of N_2 in the coupled equations of statistical equilibrium to obtain the vibrational population of each of the $B^3\Pi_g$ states. In their calculations, all of the Franck-Condon factors connecting the electronic states were those calculated by Zare[16] and by Albritton *et al.*[17] All direct-electron-excitation cross sections, except those of the W state, used in the coupling equations were the same as those reported by Cartwright.[18] In the case of the W state the direct-excitation cross sections used by Cartwright were those reported by Chutjian *et al.*[19] However, Cartwright *et al.*'s calculations indicated that radiative cascade from higher vibrational levels of the $W^3\Delta_u$ and $A^3\Sigma_u^+$ states are significant in populating the lower vibrational levels of the $B^3\Pi_g$ state.

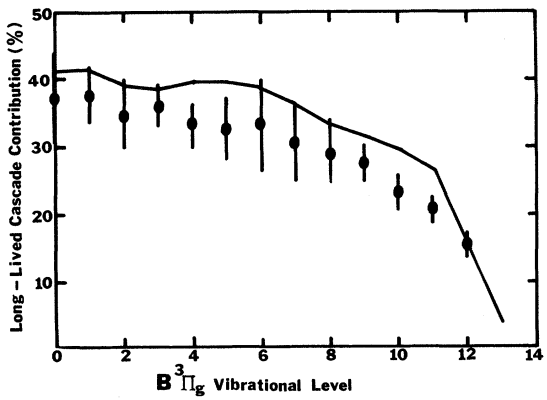

FIG. 5. Percentage contribution to the total population of the vibrational levels of the $B^3\Pi_g$ state from long-lived cascade processes: (—) the sum of $A^3\Sigma_u^+$ and $W^3\Delta_u$ cascade contribution predicted by Cartwright *et al.* (Refs. 7 and 8); (●●●) long-lived cascade contribution ($1 - N_1^*$) obtained in the present experiment including estimated reading error.

Meanwhile, Covey *et al.*[20] have pointed out that there exists a large spread in the natural lifetimes of the metastable $W^3\Delta_u$ vibrational levels. They estimated (to within 50% estimated error), that the lifetimes of the $W^3\Delta_u$ vibrational levels varied from 16.7 sec for the $v'=0$ vibrational level to 54 μsec for the $v'=7$ vibrational level. In addition, one might expect that the lifetimes could possibly be even shorter for the higher vibrational levels. The lifetime of the $v'=0$ vibrational level of the $A^3\Sigma_u^+$ state has been estimated to be 1.36 sec by Shemansky and Carleton.[21] However, since the $A^3\Sigma_u^+$ state is also a metastable state and like the $W^3\Delta_u$ state has a significant overlap of its vibrational levels with those of the $B^3\Pi_g$ state, the lifetimes of its higher vibrational levels could also be shortened as drastically as those of the $W^3\Delta_u$ state. Unfortunately, at the present time there are neither theoretical estimates nor direct measurements of the $A^3\Sigma_u^+$ high-vibrational-level lifetimes. The long-lived cascade contribution to the total population of the $B^3\Pi_g$ state observed in the present work may most likely be due to a combination of several radiative transitions from the $W^3\Delta_u$ and $A^3\Sigma_u^+$ states. Figure 5 shows the percentage contributions of the long-lived cascade contribution to the total $B^3\Pi_g$ population observed in the present experiment. These measurements are compared with the theoretical estimates of the total percentage cascade contributions from the $W^3\Delta_u$ and $A^3\Sigma_u^+$ states to the total $B^3\Pi_g$-state vibrational populations reported by Cartwright *et al.*[7,8]

Chung and Lin[4] have calculated the direct-excitation cross section of the $B^3\Pi_g$ state. They found that their calculated cross section (~$0.24a_0^2$ at 35-eV incident electron energy) was about one-half of the experimental apparent cross section[5,6] (~$0.55a_0^2$ at 35 eV) obtained after subtracting an estimated cascade contribution from the $C^3\Pi_u$ state. However, if the significant long-lived cascade contribution to the total population of the $B^3\Pi_g$ state observed in the present experiment is taken into account, the discrepancy between the theoretical and experimental values will be reduced by as much as 30%.

ACKNOWLEDGMENT

The authors wish to thank Professor R. H. Hughes of the University of Arkansas for his helpful comments and discussions during the course of this work.

*Supported in part by the Research Corporation.
[1]M. Jeunehomme, J. Chem. Phys. 45, 1805 (1966).
[2]W. Brennen, J. Chem. Phys. 44, 1793 (1966).
[3]A. Wayne Johnson and R. G. Fowler, J. Chem. Phys. 53, 65 (1970).
[4]S. Chung and C. C. Lin, Phys. Rev. A 6, 988 (1972).
[5]P. N. Stanton and R. M. St. John, J. Opt. Soc. Am. 59, 252 (1969).
[6]J. W. McConkey and F. R. Simpson, J. Phys. B 2, 923 (1969).
[7]D. C. Cartwright, S. Trajmar, and W. Williams, J. Geophys. Res. 76, 8368 (1971).
[8]D. C. Cartwright, S. Trajmar, and W. Williams, J. Geophys. Res. 78, 2365 (1973).
[9]W. R. Pendleton and R. H. Hughes, Phys. Rev. 138, A683 (1965).
[10]W. R. Pendleton, Rev. Sci. Instrum. 36, 1645 (1965).
[11]W. J. Dixon, *BMD Biomedical Computer Program X-Series Supplement* (University of California Press, Berkeley, 1970), pp. 177–186.
[12]E. R. S. Winter, Trans. Faraday Soc. 47, 342 (1951).
[13]J. B. Hasted, *Physics of Atomic Collisions* (Butterworth, London, 1964), p. 18.
[14]See E. N. Lassettre, Can. J. Chem. 47, 1779 (1969).
[15]W. B. Benesch and K. A. Saum, J. Phys. B 4, 732 (1971).
[16]R. N. Zare, Report No. 10925, Univ. of Calif. Rad. Lab., Berkeley, Calif., 1963 (unpublished).
[17]D. E. Albritton, A. Schmeltakopf, and R. N. Zare, *Diatomic Intensity Factors* (Harper and Row, New York, 1972).
[18]D. C. Cartwright, Phys. Rev. A 2, 1331 (1970).
[19]A. Chutjian, D. C. Cartwright, and S. Trajmar, Phys. Rev. Lett. 30, 195 (1973).
[20]R. Covey, K. A. Saun, and W. Benesch, J. Opt. Soc. Am. 63, 592 (1973).
[21]D. E. Shemansky and N. P. Carleton, J. Chem. Phys. 51, 682 (1969).